Polymer 50 (2009) 6121–6128

Contents lists available at ScienceDirect

Polymer

journal homepage: www.elsevier.com/locate/polymer

The melt grafting preparation and rheological characterization of long chain branching polypropylene

Shuzhao Li [a], Miaomiao Xiao [c], Dafu Wei [b], Huining Xiao [c], Fuzeng Hu [a], Anna Zheng [a,*]

[a] School of Materials Science and Engineering, East China University of Science and Technology, Shanghai 200237, China
[b] Key Laboratory for Ultrafine Materials of Ministry of Education, East China University of Science and Technology, Shanghai 200237, China
[c] Department of Chemical Engineering, University of New Brunswick, Fredericton, N.B., E3B 6C1, Canada

ARTICLE INFO

Article history:
Received 19 February 2009
Received in revised form
17 September 2009
Accepted 3 October 2009
Available online 31 October 2009

Keywords:
Polypropylene (PP)
Rheology
Melt grafting

ABSTRACT

To study the rheological properties of long chain branching (LCB) polypropylene (PP), long chain branches (LCB) were grafted onto the linear PP by melt grafting reaction in the presence of a novel chain extender, poly(hexamethylendiamine-guanidine hydrochloride) (PHGH). The branching reactions between the functionalized PP and PHGH were confirmed by transient torque curves and FTIR. By differential scanning calorimetry (DSC) and polarized microscope measurements, the presence of long chain branching structures was further confirmed. Also, the viscoelastic properties of the LCB PP and linear PP under shear flow were investigated for distinguishing LCB PP from linear PP. It was found that the elastic response of LCB PP at low frequencies was significantly enhanced in comparison with that of the linear PP, implying a presence of a long relaxation time mode that was not revealed in linear PP. Moreover, the branching levels of LCB PP were quantified using a detailed method, which was in correspondence with the molar amount of PHGH grafted on PP.

1. Introduction

Polypropylene, one of the most widely used thermoplastics, is the fastest growing commodity resin in the polymer world market. PP possesses many excellent properties, such as good heat and chemical resistance, high melting temperature and stiffness, low density and reusability. Various methods have been applied to PP fabrications, such as injection molding, film extrusion, and compression. However, PP exhibits low melt strength and weak strain hardening behavior because it is one of these polymers with highly linear chains and a relatively narrow molecular weight distribution (MWD), which limits its applications in foaming, blow molding, thermoforming and spinning. For the improvement of melt properties, such as melt strength and strain hardening behavior, many attempts have been performed by some researchers. The melt strength of PP can be improved by many methods such as increasing the molecular weight, broadening the distribution or introducing branches. Even, High melt strength PP (HMS PP) can be prepared only by adding or grafting some inorganic nanofillers in PP matrix, such as silica, organoclay and carbon nanotube, etc. [1–5]. The significant change in the viscoelastic properties results from the incorporation of nanofillers well dispersed in molten polymers [1,2]. Therefore, to well disperse the nanofillers into PP, the nanofillers have to be chemically modified due to their fractal structure and high specific surface area; after all, rheological properties depend on both the state of dispersion of the fillers and the presence of chemical bonding [3]. In addition, Gotsis and Zeevenhoven [6] have shown that large enhancements of the melt strength of PP were achieved by the introduction of high molecular weight polyethylene (PE) into PP in the polymerization process with a heterogeneous catalyst. Also, by using atom transfer radical polymerization, Zhai et al. [7] synthesized isotactic polypropylene copolymers grafted by polystyrene (PS) and poly(methyl methacrylate) (PMMA) with well-defined chain structure. Whereas, as described in his work, PMMA-rich dispersed phase can be observed due to the poor compatibility with PP, implying that the compatibility with PP has to be taken into consideration when introducing heterogeneous polymers onto PP. Compared with this method, introducing branches onto the backbone of commercial PP via some post-reaction modifications seems to be a more efficient approach due to its accessibility to industrialization and less cost.

Several commercial HMS PP grades have been achieved, wherein, most of them were developed using the electron beam (EB) irradiation [8]. By EB irradiation, HMS PP is commercially

* Corresponding author. Tel.: +86 21 64253343; fax: +86 21 64252744.
E-mail address: zan@ecust.edu.cn (A. Zheng).

0032-3861/$ – see front matter © 2009 Elsevier Ltd. All rights reserved.
doi:10.1016/j.polymer.2009.10.006

Table 1
Polymers used in the present work.

Code	GMA content (g/100 g PP)	M_w	M_w/M_n	T_m (°C)[a]	Melt strength (N)[b]	MFI (g/10 min)
EPS	0	398,000	4.50	161.1	0.3	2.7
PP-GMA-1	0.10	367,000	4.57	–	–	2.7
PP-GMA-2	0.20	352,000	4.65	–	–	2.6
MPP-1	0.10	432,000	5.01	160.3	0.86	2.1
MPP-2	0.20	497,000	5.37	157.9	0.91	1.5

[a] Melt temperature was obtained from DSC measurements.
[b] Melt strength was measured at 180 °C.

available (e.g., Profax® by Basell and Daploy® by Borealis) and has been successfully used in foaming, thermoforming and extrusion coating processes. However, the EB irradiation causes β-scission of the PP chains followed by crosslinking [9–12]. Furthermore, the chain branches produced by EB irradiation are confined in the amorphous phase of the semicrystalline PP, which will limit the numbers of chain branches. Also, many publications described the modification of PP with peroxides in combination with multi-functional monomers [13–16]. Wang [15] and Tian [16] reported the possibility of producing branched PP by reactive extrusion in the presence of pentaerythritol triacrylate (PETA) combined with 2,5-dimethyl-2,5(*t*-butylperoxy) hexane peroxide. The extrusion of PP with peroxydicarbonates (PODIC) has been patented by Basell [17] and by Akzo-Nobel [18,19]. However, the limitation of this method is also obvious. There are unavoidable degradation and crosslinking apart from branching reactions during the extrusion process [14].

Wang et al. [20] blended acrylic acid-grafted PP with alkyl amines via reactive extrusion and prepared a HMS PP with higher zero-shear viscosity, high modulus and lower glass transition temperature. In their report, the content of formed imide was increased with increasing the reaction time up to 10 h, while a further increase in reaction time resulted in a reversal reaction. However, such long reaction time (e.g. 10 h) made it impossible for reactive extrusion. In addition, these compounds grafted onto the backbone of PP as the chain branches are too short to producing a satisfying HMS PP. Some researchers utilized a functionalized PP, such as amine functioned PP [21], and a polyfunctional compound to prepare HMS PP. Kim [22] reported that enhanced melt strength was obtained by reactive extrusion of randomly functionalized PP with polyfunctional compound, while higher gel content was accompanied during the process. Reactive extrusion of functionalized PP with polyfunctional compounds is supposed to be a better approach to produce HMS PP in the event of avoiding gel because it can produce longer and homogeneous branching chains onto the backbone of PP, consequently substantially increasing the melt strength of PP. Lu and Cao [23] used supercritical CO_2 ($ScCO_2$) to prepare LCB PP in melt reaction system consisting of diethylamine (DEA) and functionalized PP grafted by maleic anhydride (PP-g-MAH). The use of $ScCO_2$ helps to improve the flow properties and decrease the melt viscosity of the reaction system distinctly. Therefore, the branching reaction can take place in the system, abating the influence of mass transfer usually taking place in macromolecule reactions.

In this work, LCB PP was prepared by melt grafting in the presence of glycidyl methacrylate-grafted PP (PP-GMA) and a novel chain extender, PHGH, which helps to decrease the melt viscosity and improve the reaction activity. One of the objectives of our current work is to develop a feasible reactive extrusion by melt grafting for increasing the melt strength of commercial linear PP, thereof avoiding the formation of gels owing to the controllability of the branching level of LCB. Additionally, rheological measurements were performed to investigate the influence of LCB structures on melt behaviors and distinguish LCB PP from linear PP.

2. Experimental

2.1. Materials

The commercial PP, EPS (EPS30R, Qilu Petrochemical Co.), is linear PP. PP-GMA-1 and PP-GMA-2 are intermediate products grafted by various concentration of glycidyl methacrylate (GMA) on the backbone of EPS and supplied by Shanghai Fuyuan Co. The amount of GMA in PP-GMA-1 and PP-GMA-2 is listed in Table 1. The novel chains extender, PHGH ($M_W = 800$, Fuyuan Co., Shanghai), is an oligomer with lower melt temperature, and its structure is shown in Scheme 1, where n and m is the degree of polymerization, and Y stands for anion, such as Cl^-, NO_3^- and HCO_3^-.

2.2. Preparation of samples

The preparation of HMS PP took place in a Haake Rheomin 600p mixer at 180 °C and 60 rpm for 5 min. The premix of PP-GMA-1, PHGH and 0.2% antioxidant, Irganox 1010 (Ciba), which was mixed in a high speed mixer in advance, was added into the Haake mixer to prepare the MPP-1 sample. The MPP-2 sample was prepared by PP-GMA-2 and PHGH using the same method. The properties of modified PP, MPP-1 and MPP-2, are listed in Table 1, and the formulations are listed in Table 2.

2.3. Characterization

The melt strength of all PP samples was measured using a Gottfert Rheotens Melt Strength Tester consisting of a pair of rollers rotating in opposite directions. Samples strand extruded vertically downwards from a capillary die is drawn by the rotating rollers whose velocity increases at the constant acceleration rate of 20 mm/s^2. The tensile force in the strand measured by the balance beam is called the melt strength when the polymer melt breaks.

The number average molecular weight $\overline{M}_n$, the weight average molecular weight $\overline{M}_w$ and the MWD ($\overline{M}_w/\overline{M}_n$), were determined via a high temperature size exclusion chromatography at 150 °C (Waters 150C gel permeation chromatography, PS gel columns). PP sample (0.1 g) was dissolved in 100 mL of ortho-di-chlorobenzene containing 0.1 wt% butyl hydroxyl toluene. Their molecular weight was calculated in a standard procedure based on universal calculation of PP.

Flow properties of all PP samples were measured using a SRSY-1 capillary rheometer. The melt flow index (MFI) of all polymers was measured at 230 °C using a load of 2.16 kg according to the ASTM D-1238-86T standard.

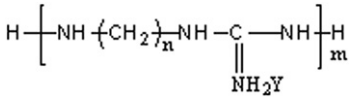

Scheme 1. Chemical structure of PHGH.

Table 2
The formulations and abbreviations of samples.

Samples	PP-GMA (g)		PHGH[a] (g)	Irganox 1010 (g)
	PP-GMA-1(g)	PP-GMA-2(g)		
MPP-1	100	–	0.28	0.2
MPP-2	–	100	0.57	0.2

[a] The GMA-to- PHGH molar ratio is 2:1.

For FTIR spectroscopy, the modified sample was dissolved in hot xylene at 140 °C, and then the solution was poured into enough methanols at room temperature. Here, linear PP and modified PP precipitated out, and the unreacted residual PHGH remained in the mixed solution. The purified PP was obtained by filtration and dried at 80 °C under vacuum for 24 h. At last the purified and unpurified samples were analyzed using Nicolet AVATAR 360 FT-IR.

DSC analysis was carried out with a TA Instruments thermoanalyzer equipped with a 2910 differential scanning calorimetric. The measurement was performed at a heating rate of 10 °C/min under a dry nitrogen atmosphere. For removal of the thermal history, after the sample cell was heated from the room temperature to 200 °C, the temperature was hold for 10 min and then cooled to the room temperature. For the melting test, a second run was made at a heating rate of 10 °C up to 200 °C immediately after the first run was completed.

The crystal morphology of all PP samples were studied using a polarized microscope attached on a LV100POL optical rheology microscope (Nikon Corporation) with a Cryo-CSS450 heating and cooling platform (Linkam Scientific Instruments Ltd) from −50 to 450 °C. EPS and modified PP were heated to 200 °C at 20 °C/min and kept for 5 min at 200 °C to eliminate the thermal history. They were then crystallized non-isothermally from 200 °C to 25 °C, decreasing 20 °C/min.

The modified samples were cut into small pieces and packed with filter paper, respectively, and then were Soxhlet extracted in boiling xylene for 24 h. No gel was observed for all modified samples.

Shear dynamic measurement was carried out with a Rheostress 600 rotational rheometer manufactured by Haake Co. The parallel plate with a diameter of 25 mm and a gap height of 2 mm was used for frequencies sweeps. The test specimen was cut from a sheet that has been prepared by compression molding at 180 °C. The range of the frequency sweeps was from 0.001 rad/s to 100 rad/s, and a strain of 1% was used, which was in the linear viscoelastic regime for all samples. The shear dynamic measurement was carried out at a constant temperature of 180 °C while dry nitrogen was maintained to keep oxygen out for avoiding oxidative degradation of the polymers during the measurement. The values of storage modulus G' and loss modulus G'' against the frequencies were obtained in the results.

3. Results and discussion

3.1. Reaction in Haake, torque curves and GPC traces

As shown in Scheme 2, PP-GMA macromolecules were coupled by the novel chain extender, PHGH, to form branching macromolecules. The modified PP samples shown in Scheme 2 are star-type or comb-type topological structures varying with the concentration of GMA grafted on PP.

Fig. 1 shows the transient torque trace of the grafting reaction between PP-GMA and PHGH. For the EPS sample, the torque curve keeps nearly horizontal after complete melting. However, for the torque curves of PP-GMA/PHGH systems, the second peak appears at about 2.2 min besides the melting peak. Moreover, the second peak becomes higher with the increase of PHGH concentration, implying that branching reactions took place in the system. In fact, no gel was detected in two HMS PP samples. Therefore, the increase of the torque, corresponding to the increase of viscosity, can be attributed to the grafting reactions of PP chains. Although some diamine compounds, such as hexamethylendiamine and butanediamine, were used as chain extenders to react with functionalized PP by some researchers [22], the problem of mass transfer, which usually takes place in macromolecular reactions, can influence its practical application in melt grafting reactions. Therefore, the modification of PP by this method has only been carried out in solvent for studying the controllability of molecular structures. In our reaction systems, PHGH acts as a plasticizer due to its lower viscosity, which can improve the flow properties of PP matrix and help the branching reactions.

That LCB are generated can be deduced from the GPC results. Fig. 2 shows the MWD curves for the samples of EPS, PP-GMA-2 and MPP-2. In the MWD curve of MPP-2, a small shoulder that is seen at the higher molecular mass region and which is not revealed in EPS and PP-GMA-2 samples could be interpreted as a broadening of the distribution because of the branching reactions. In the present case, this widening is most likely due to the existence of LCB molecules.

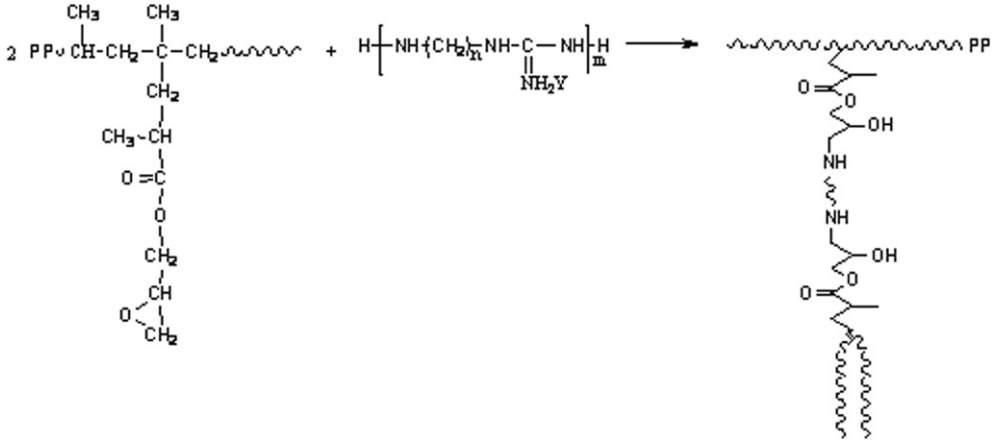

Scheme 2. Formation and microstructure of modified PP.

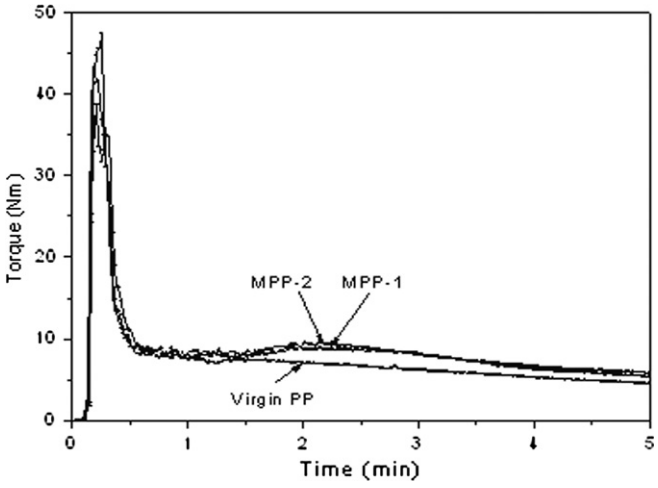

Fig. 1. Transient torque curves of virgin PP and modified PPs.

3.2. FTIR spectroscopy

To achieve the grafting efficiency of PHGH, FTIR measurements of EPS and modified samples were performed. Fig. 3 shows the FTIR spectra of EPS and MPP-1. For the MPP-1 sample, a new band appears at about 1640 cm^{-1} which is attributed to the stretching vibration of the imine groups in the PHGH molecules, indicating that PHGH was grafted onto the PP backbone. However, from Fig. 3 it can be seen that the absorbance peak at 1640 cm^{-1} for purified MPP-1 decreases in comparison with unpurified MPP-1, implying that not all of the PHGH was grafted onto the backbone of PP. Through the FTIR spectra, the absorbance, A, can be calculated by Lambert–Beer's law expressed by Equation (1) [24],

$$A = \varepsilon lc = -\log\frac{I}{I^0} \tag{1}$$

where I^0 is the intensity of incident radiation on the sample, and I is the intensity through the sample of length l and concentration c. ε is the absorptivity. To achieve the grafting efficiency of PHGH, a referential peak located at 1380 cm^{-1} in the present case is needed. Therefore, the ratio of the imine absorbance at 1640 cm^{-1} and the methyl band at 1380 cm^{-1}, R_S, is used to determine the composition of the sample and calculated as follows [25,26],

$$R_S = \frac{A_{NH}}{A_{CH_3}} \tag{2}$$

where A_{NH} and A_{CH_3} are the absorbance of imine and methyl groups respectively through the sample of length l and concentration C_{NH} or C_{CH_3}. In addition, to achieve the grafting efficiency of PHGH, a calibration curve is needed. The blends with known amount of PHGH over the range of about 0–20 wt% were prepared in Haake mixer. The grafting efficiency was then calculated and listed in Table 3. It can be seen that more PHGH was grafted onto MPP-2 compared with MPP-1, implying that the branching degree of MPP-2 increases. The result is in agreement with the analysis of the torque curves. Furthermore, x value, i.e., the fraction of LCB in all chains, can be achieved by calculating the molar amount of PHGH grafted on PP. The x values are listed in Table 3.

3.3. Analyses of DSC and crystal morphology

Fig. 4 shows the melting and crystallization behaviors of the linear PP and modified samples by DSC. It can be seen that the melting and crystallization temperatures of modified PPs are apparently different from those of the linear PP, EPS. For modified PPs, the melting temperature decreases, and the crystallization temperature increases due to the introduction of branching structures on the PP chains compared with EPS. Furthermore, with the increase of branching structures, for MPP-2 the melting temperature becomes lower, and the crystallization temperature becomes higher in comparison with MPP-1. In addition, in Fig. 4, the heat of fusion, ΔH, of modified PP decreases as compared with that of EPS, which also suggests that the crystallinity degree of modified PP decreases due to the increase of branching structures.

The crystallization processes and crystal morphologies of EPS, PP-GMA-1 and MPP-1 can be clearly observed using a polarized microscope attached on an optical rheology microscope. Fig. 5 shows the micrographs of linear PP (EPS and PP-GMA-1) and MPP-1, which was crystallized non-isothermally from 200 °C to 25 °C, decreasing 20 °C/min. From Fig. 5 it can be clearly seen that the crystallization of linear PP and modified PP is significantly different. For linear PP, EPS and PP-GMA-1, the crystal morphologies are global crystals with the phenomenon of Maltese Cross extinction (A and B in Fig. 5). However, for MPP-1, an abundant of irregular crystals were formed instead of normal global crystals (C in Fig. 5), which implies that the LCB on the modified PP perform the function of heterogeneous nucleation. Moreover, by observing the process of

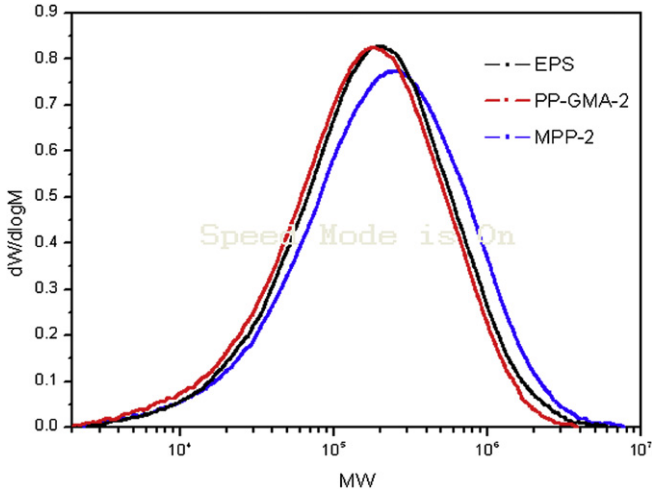

Fig. 2. MWD curves of original PP and modified PPs.

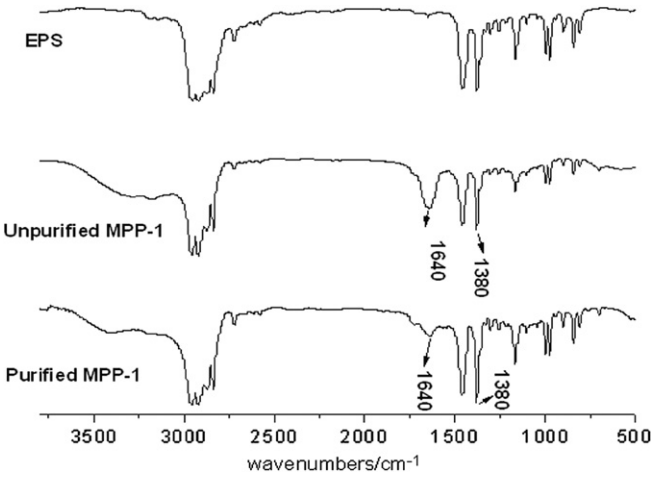

Fig. 3. FTIR spectra of some PP samples.

Table 3
Rheological parameters of the linear PP and HMS PP.

Sample	Grafting efficiency (wt%)	x	η_0 ($\times 10^4$ Pa.s)	λ (s)	n	Terminal slop of G'	B_n
PP	–	–	1.19	1.43	0.71	1.33	0
PP-GMA-1	0	0	0.48	0.76	0.73	1.48	0
MPP-1	82.1%	0.19	1.38	20.40	0.43	0.78	0.11
MPP-2	83.3%	0.36	2.29	441	0.39	0.57	0.38

non-isothermal crystallization of all samples, it can be found that for MPP-1 most of the crystal nuclei were generated instantaneously, implying that the introduced branching structures speeded up the nucleation. However, the growth rate of its crystals decreases because the chains transfer from the PP melt to the crystallization interface is restrained by the LCB. On the other hand, for EPS the crystal nuclei were generated slowly due to the homogeneous nucleation, differing from the conjunction of simultaneous heterogeneous and homogeneous nucleation in MPP-1. As a whole, the crystallization rate of modified PP increases in comparison with that of linear samples as shown in B, D and E of Fig. 5. At 110 °C, i.e. in the same time, for the MPP-1 the crystallization process came to an end, however, single crystals can still be observed in B and D of Fig. 5, especially, for PP-GMA-1. The results are in correspondence with the results of DSC, further indicating that the introduction of LCB advances the crystallization.

3.4. Linear viscoelastic properties

Linear viscoelastic properties are very sensitive to the structural change of the materials. Also, it has proved to be a reliable method for verification of existence of LCB on polymeric chains and it is easier to implement [27]. It will be demonstrated below from different rheological plots that the melt grafting reactions in the PP systems can result in new topological structures with longer relaxation time, which is ascribed to the molecules with LCB.

The complex viscosity curves of all PP samples at 180 °C are shown in Fig. 6. For linear PP, EPS, the complex viscosity becomes independent of the frequency at low frequencies, in correspondence to Newtonian-zone. When only GMA was grafted onto PP (sample PP-GMA-1), complex viscosity decreased severely at low frequency and Newtonian-zone became broader, implying that β-scission took place and the molecular weight decreased although GMA was grafted on the backbone of PP. With the LCB increasing, the complex viscosity of modified PP, MPP-1 and MPP-2, at low frequency increases gradually, especially for MPP-2, whose terminal value is beyond that of EPS. Furthermore, the transition from Newtonian-plateau to shear-thinning regime is shifted to lower frequency. The presence of very low amounts of LCB can change the zero-shear viscosity (η_0) and the degree of shear thinning, as compared with the linear polymers with similar molecular weight [28]. The complex viscosity of the samples can be fitted by the cross equation [29], which is written as,

$$\eta^*(\omega) = \frac{\eta_0}{1 + (\lambda\omega)^n} \tag{3}$$

where η_0 is the Newtonian viscosity, λ is the cross time constant whose reciprocal accounts for the onset of shear-thinning region and n is a shear-thinning index. These values for the linear PP and modified PPs are listed in Table 3. It can be seen that with the addition of PHGH, the rheological parameters changes regularly, i.e., η_0 and λ increase and n decreases. Therefore, the effect of branches on viscosity is clear that there is no evident Newtonian-plateau at low frequency and the shear thinning starts at lower frequency than that of the linear PP. Similar result was also obtained by Sugimoto et al. [30].

Besides zero-shear viscosity, the storage modulus and the loss angle are even more sensitive to LCB [31]. In the terminal flow region, where only the longest relaxation time contributes to the viscoelastic behavior, G' and G'' are proportional to ω^2 and ω respectively according to the well-known frequency dependence [32].

Fig. 7 shows G' plotted as a function of frequency for all PP samples. It can be seen that, in comparison with that of EPS, G' of MPP-1 and MPP-2 is significant higher at low frequency (terminal zone) and slightly lower at relatively high frequency. In Fig. 7, EPS and PP-GMA-1 exhibit the typical terminal flow behavior, indicating they are linear PP. However, the modified PP samples deviate from the terminal behavior. With the addition of PHGH, the terminal slope of G' decreases from 1.33 of the linear PP to 0.57 of MPP-2 (Table 3), suggesting that the HMS PP shows non-terminal behavior. Furthermore, the height of the shoulder of HMS PP increases with the increase of the branching structures. The non-terminal behavior of HMS PP implies that there is a longer relaxation mechanism, which can be ascribed to the LCB formed from the melt grafting reactions.

Fig. 8 exhibits an increase in the elastic response at low frequency of HMS PP (MPP-1 and MPP-2), that is, a decrease in tan δ. With frequency decreasing, tan δ curves of MPP-1 and MPP-2 culminate in the vicinity of 0.04 rad/s, whereas those of EPS and PP-GMA-1 keep rising highly which is the typical terminal behaviors of liquid-like materials. Furthermore, with LCB increasing, tan δ decreases quickly at low frequency and shows a plateau. For MPP-2, the tan δ decreases continually, and the plateau becomes longer. This result is in accordance with the result of Graebling [33], who attributed this to the grafting of LCB on the PP skeleton and increasing the terminal relaxation time.

The non-terminal behaviors of the modified PP samples can also be illustrated in the Han plot ($\log G' - \log G''$, Fig. 9) and Cole–Cole plot ($\eta'' - \eta'$, Fig. 10). The Han plot has been used to investigate

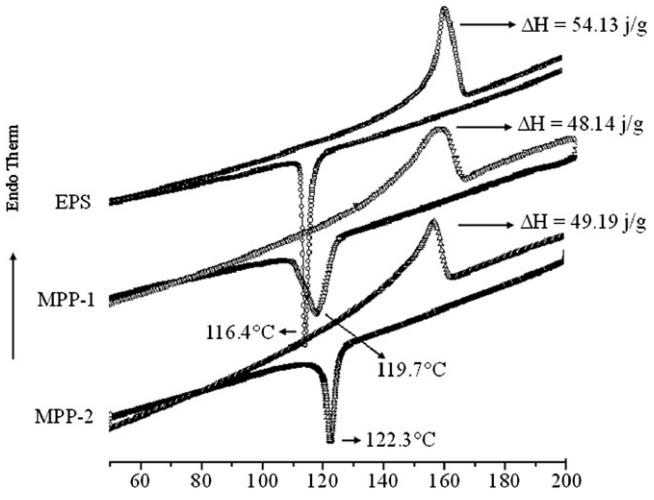

Fig. 4. DSC of linear PP and modified PPs.

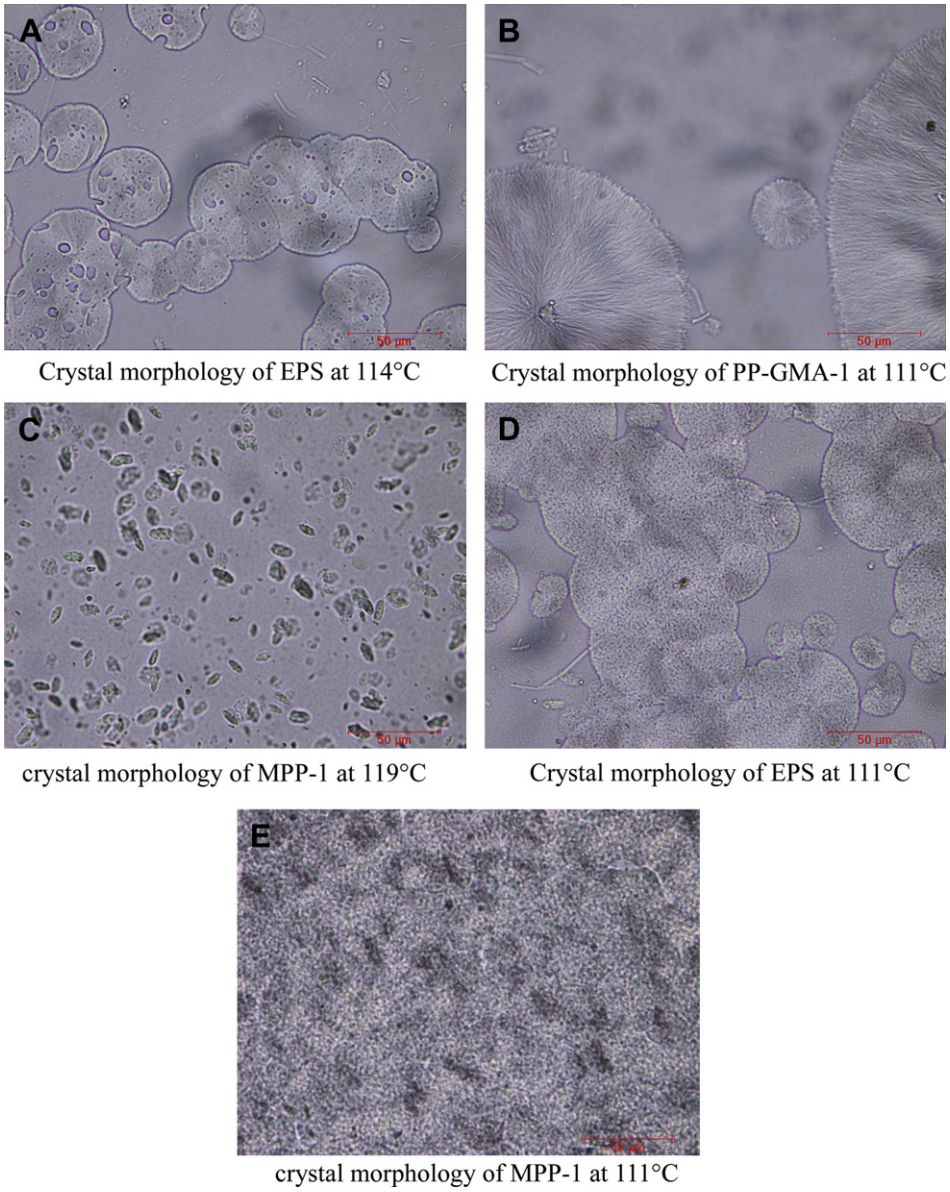

Fig. 5. Crystal morphologies of linear PPs and modified PP.

order-disorder transition in block copolymers [34,35], the effect of polydispersity and LCB in polyethylenes [36] and miscibility of polymer blends [37,38]. Han plot is independent of the melt temperature and weight average molecular weight for monodispersed polymers. For PE with shorter branching chains or narrow MWD, the relation between G' and G'' is [36]: $G'=0.00541(G'')^{1.42}$. However, the Han plot will deviate from the curve for PE with LCB or wide MWD. As shown in Fig. 9, the Han plots of EPS and PP-GMA-1 are almost linear and their formulas are $\lg G' = -2.01 + 1.45 \lg G''$ and $\lg G' = -2.38 + 1.5 \lg G''$ respectively, implying that EPS and PP-GMA-1 are linear. The Han plots of modified PPs, MPP-1 and MPP-2, deviate up significantly from the linear plot of EPS at lower frequencies, indicating that a long relaxation mechanism occurred in theses samples. Furthermore, with the LCB increasing, the deviation apparently increases, implying that the contribution of elasticity in the modified samples is more than that of viscosity.

The long relaxation process of modified PP samples can also be seen in the Cole–Cole plot (Fig. 10). As shown in Fig. 10, the

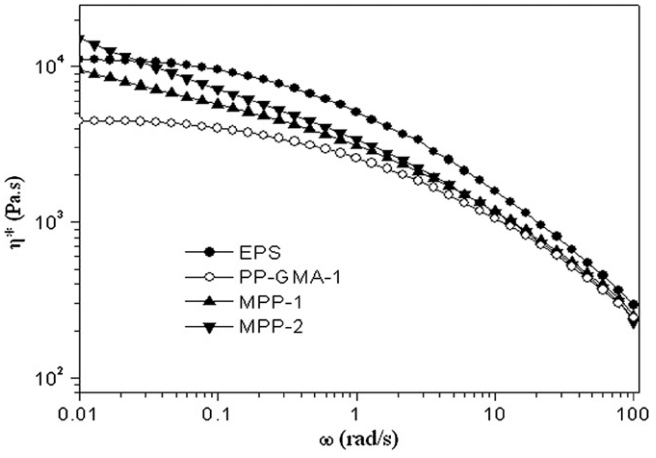

Fig. 6. Complex viscosity vs. angle frequency for the linear PP and modified PP samples at 180 °C.

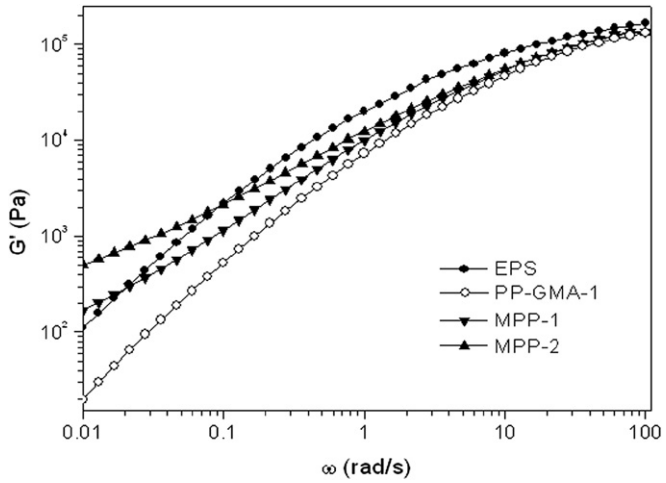

Fig. 7. Storage modulus vs. angle frequency for the linear PP and modified PP samples at 180 °C.

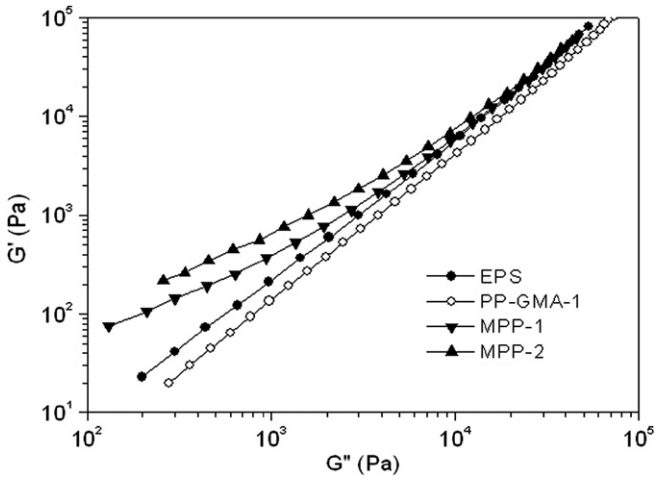

Fig. 9. Storage modulus vs. loss modulus for the linear PP and HMS PP samples at 180 °C.

differences of theses samples are very clear. For EPS and PP-GMA-1, the Cole–Cole plot is close to a semicircle, and the higher the molecular weight is, the bigger the radius is. The curves of MPP-1 and MPP-2 are higher than that of the linear PP and show a drastic upturning at high viscosity corresponding to lower frequency. And the more LCB are, the higher the deviation is, indicating that a longer relaxation time appears.

Loss angle, δ, can be used to evaluate the structures of polymers with LCB by Van Gurp–Palmen plotted as a function of the absolute value of complex modulus ($|G^*(\omega)|$). vGP plot was proposed by Van Gurp and Palmen [39] and used to prove the validity of time–temperature superposition principle. Subsequently, Trinkle [40] et al. found that the plot includes some information about molecular structures in linear polymers, such as molecular weight, MWD and LCB etc.

Fig. 11 shows that the δ values of EPS and PP-GMA-1 are increasing with $|G*(\omega)|$ decreasing, especially for PP-GMA-1, whose terminal value of δ is close to 90°. However, when LCB structures are introduced into the PP backbone, the vGP plot of HMS PP, MPP-1 and MPP-2, deviate from the curve of linear PP. The δ values of modified PP samples are lower than that of EPS almost in all scope of the measurement, especially, in the lower frequency. Furthermore, the δ value at lower frequency and the area enwrapped by the curve decrease with the increase of the LCB structures. Materials are almost completely viscous when the δ value is close to 90° and almost completely elastic when the δ value is close to 0° [41]. Therefore, from Fig. 11, it can be seen that the elasticity of HMS PP is higher than that of EPS and PP-GMA-1, and the elasticity of HMS PP increases with LCB increasing. Lohse [41] found that the vGP plots of star-type and comb-type branched PE are evidently different: in the vGP plot of star-type PE, the δ value decreases with the increase of $|G*(\omega)|$ until close to 0°; however, for comb-type PE, a semicircle appears before δ is close to the minimum value although it also decreases with the increase of $|G*(\omega)|$. Therefore, according to the characteristic of melt grafting and the vGP plot shown in Fig. 11, it can be conjectured that MPP-1 and MPP-2 are star-type topological structures.

3.5. Quantitative analysis of LCB

Determination of the level of LCB in polymers is not an easy task, and several methods were proposed by some researchers [16,42–45], and even more difficult in our system due to the complex reactions that happened during the modifications of PP. Tsenoglou and Gotsis [42] have shown that the zero shear viscosity, η_0, of the melt was increased by the introduction of sparse LCB on linear PP

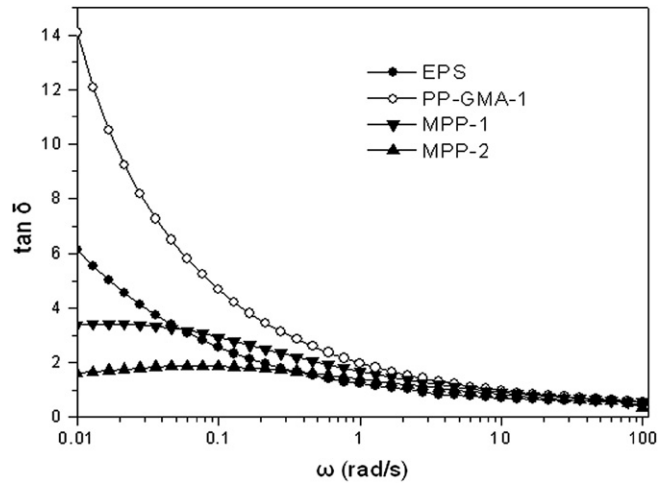

Fig. 8. Tan δ vs. angle frequency for the linear PP and modified PP samples at 180 °C.

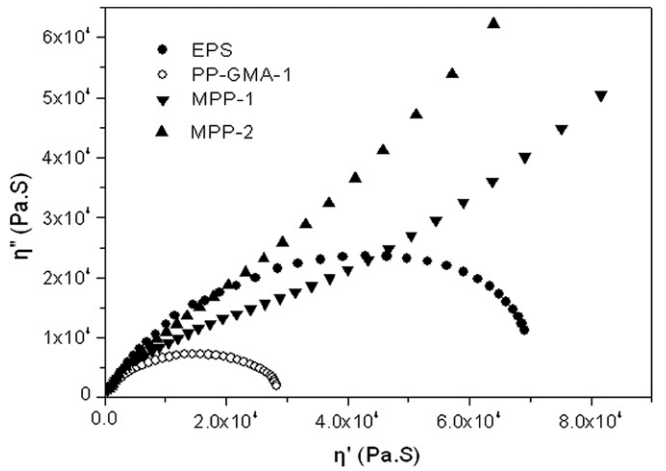

Fig. 10. Cole–Cole plot of the linear PP and modified PP samples at 180 °C.

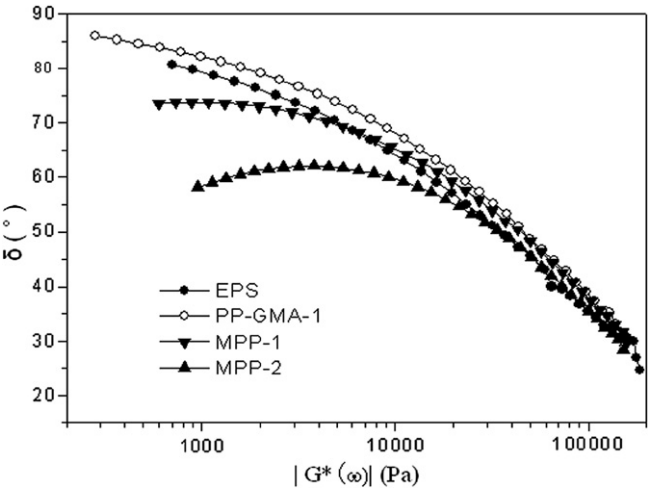

Fig. 11. vGP plot of the linear PP and HMS PP samples at 180 °C.

chains at (almost) constant weight average molecular weight, M_w, something that is not true for broadening the MWD. The increase of $\eta_{0,LCB}$ is related quantitatively to B_n.

$$B_n \approx \frac{\ln\left(\frac{\eta_{0,LCB}}{\eta_{0,L}}\right)}{\alpha\left(\frac{M_W}{M_C}-1\right)-3\ln\left(\frac{M_W}{M_C}\right)} \quad (4)$$

where, M_C is the molecular weight at the onset of entanglements and equal to 13640 g/mol for PP [46], and α is a constant ($\alpha = 0.42$). $\eta_{0,LCB}$ is the zero-shear viscosity of branched and linear blend, $\eta_{0,L}$ and M_W are the zero-shear viscosity and the weight average molecular weight of the original PP. The method works only for polymers where the branches are the same as the backbone (same chain flexibility), where there are no significant changes of the molecular weight upon modification, and for $B_n \ll 1$ [47]. It should be noted here that Equation (4) can be used only when $\eta_{0,LCB}$ is higher than $\eta_{0,L}$. Therefore, for our modified PP samples, the branching level can be calculated by Equation (4). The values of B_n for MPP-1 and MPP-2 were listed in Table 3. As shown in Table 3, for MPP-1 and MPP-2, the values of B_n are close to the value of x, implying that the two methods to qualify the branching levels of modified PP are feasible for our reaction systems. These results also show that the branching density of modified PP increases with the addition of PHGH concentration.

From above discussion, it is clear that a longer relaxation process appeared in the modified PPs with LCB. It is believed that this longer relaxation process is related to LCB that results from the melt grafting reaction.

4. Conclusions

In this study, HMS PPs were prepared by melt grafting reaction in the presence of a novel chain extender, PHGH, and PP-GMA. Rheological behaviors of the linear PPs and modified PPs were investigated in detail by several rheological plots. Moreover, the level of LCB was quantified by calculating the amount of PHGH grafted on PP.

Branching reactions could take place in the Haake mixer, which was verified by the torque curves and FTIR spectra. The formation of branching structure was confirmed by DSC, polarized microscopy and small-amplitude oscillatory shear experiments. The melt temperature and crystal morphologies of HMS PP were evidently different from that of linear PP due to the introduction of LCB based on DSC and polarized microscopic measurements. Several rheological plots were used to investigate the rheological behaviours of the linear PP and HMS PP. The rheological properties of HMS PP were different from those for linear PP, such as higher G' at lower frequency, plateau in tan δ–ω plot, deviating from the scaling G'–G''^2 of linear polymer in Han plot, upturning at high viscosity in Cole–Cole plot, and close to 0°at low frequency in vGP plot. The results revealed the different relaxation mechanism for HMS PP from that for linear PP.

References

[1] Alberto F, Daniela T, Ton P, Giovanni C. Polymer 2009;50:218–26.
[2] Cassagnau Ph. Polymer 2008;49:2183–96.
[3] Mathieu B, Marianna K. Polymer 2009;50:2472–80.
[4] Geon-Woong L, Sudhakar J, Han GC, Marilyn LM, Satish K. Polymer 2008;49:1831–40.
[5] Xu DH, Wang ZG. Polymer 2008;49:330–8.
[6] Gotsis AD, Zeevenhoven BLF, Hogt AH. Polymer Engineering and Science 2004;44(5):973–82.
[7] Zhai WT, Wang HY, Yu J, Dong JY, He JS. Polymer 2008;49:3146–56.
[8] Manfred R. Journal of Macromolecular Science Part A 1999;36(11):1759–69.
[9] Scheve BJ, Mayfield JW. Denicola JR. Himont Inc. US Patent 4,916,198, 1990.
[10] Denicola JR. Himont Inc. E. Patent 0383431B1, 1989.
[11] Yoshii F, Makuuchi K, Kikukawa S, Tanaka T, Saitoh J, Koyama K. Journal of Applied Polymer Science 1996;60(4):617–23.
[12] Bennie ML, Krishnamurthy V, John RB. Rexene Corporation (Dallas, TX), US Patent 5,439,949, 1995.
[13] Parent JS, Aidan B, Saurav SS, Marianna K, Bharat IC, Drew P, et al. Polymer 2009;50:85–94.
[14] Parent JS, Saurav SS, Michael K, Bharat IC. Polymer 2008;49:3884–91.
[15] Wang XC, Tzoganakis C, Rempel GL. Journal of Applied Polymer Science 1996;61(8):1395–404.
[16] Tian JH, Yu W, Zhou CX. Polymer 2006;47:7962–9.
[17] Denicola JR. Himont Inc. E Patent 0383431B1, 1989.
[18] Hogt AH, Westmijze H. WO Patent 9,749,759, 1996.
[19] Hogt AH, Fischer B, Spijkerman GK. WO Patent 9,927,007, 1999.
[20] Wang XC, Tzoganakis C, Rempel GL. Annual Technical Conference Society of Plastics Engineers 1994; 52nd(2):1449–55.
[21] Cui LL, Paul DR. Polymer 2007;48:1632–40.
[22] Kim KY, Kim SC. Macromolecular Symposia 2004;214(1):289–97.
[23] Lu W, Cao K, Yao Z. 4th East Asia Polymer Conference 2006; Tianjin:131–132.
[24] Xie JX. Use of infrared on organic chemistry & medicament chemistry. 1st ed. Beijing: Science Press; 1987. pp. 32–34.
[25] Levin RM. Journal of the Electrochemical Society 1982;129(8):1765–70.
[26] Levin RM, Adams AC. Journal of the Electrochemical Society 1982;129(7):1588–92.
[27] Gotsis AD, Zeevenhoven BLF, Hogt AH. Polymer Engineering and Science 2004;44(5):973–82.
[28] Anneli M, Claus G, Thomas S, Helmut M, Barbro L. Macromolecules 2002;35(3):1038–48.
[29] Kolodka E, Wang WJ, Zhu SP, Archie EH. Macromolecules 2002;35(27):10062–70.
[30] Sugimoto M, Tanaka T, Masubuchi Y. Journal of Applied Polymer Science 1999;73(6):1493–500.
[31] Wood-Adams PM, Dealy JM. Macromolecules 2000;33(20):7481–8.
[32] Ruymbeke EV, Stephenne V, Daoust D. Journal of Rheology 2005;49(6):1503–20.
[33] Graebling D. Macromolecules 2002;35(12):4602–10.
[34] Choi S, Han CD. Macromolecules 2002;37(1):215–25.
[35] Antony P, Puskas JE. Polymer Engineering Science 2003;43:243.
[36] Vega JF, Santamaria A, Munoz-Escalona A, Lafuente P. Macromolecules 1998;31(11):3639–47.
[37] Han CD. Journal of Applied Polymer Science 1988;35(1):167–213.
[38] Chopra D, Kontopoulou M, Vlassopoulos D, Hatzikiriakos SG. Rheologica Acta 2002;41:10–24.
[39] Gurp van M, Palmen J. Rheology Bulletin 1998;67:5–8.
[40] Trinkle S, Walter P, Friedrich C. Rheologica Acta 2002;41:103–13.
[41] Lohse DJ, Milner ST, Fetters LJ, Xenidou M, Hadjichristidis N, Mendelson RA, et al. Macromolecules 2002;35(8):3066–75.
[42] Tsenoglou CJ, Gotsis AD. Macromolecules 2001;34(14):4685–7.
[43] Janzen J, Colby RH. Journal of Molecular Structure 1999;84:569–84.
[44] Shaw MT, Tuminello WH. Polymer Engineering Science 1994;34(2):159–65.
[45] Wood-Adams PM, Dealy JM. Macromolecules 2000;33(20):7481–8.
[46] Langston JA, Colby RH, Chung TCM, Shimizu F, Suzuki T, Aoki M. Macromolecules 2007;40(8):2712–20.
[47] Borsig E, Duin vM, Gotsis AD, Picchioni F. European Polymer Journal 2008;44:200–12.